applied sciences

MDPI

Article

Real-Time Monitoring of Occupational Radiation Exposure in Nuclear Medicine Technologists: An Initial Study

Masaki Fujisawa [1,*], Masahiro Sota [1,2], Yoshihiro Haga [1,2], Shigehisa Tanaka [2], Nozomi Kataoka [2], Toshiki Kato [1,2], Yuji Kaga [2], Mitsuya Abe [2], Masatoshi Suzuki [1,3], Yohei Inaba [1,3] and Koichi Chida [1,3,*]

[1] Course of Radiological Technology, Health Sciences, Tohoku University Graduate School of Medicine, 2-1 Seiryo, Aoba-ku, Sendai 980-8575, Japan; masahiro.st63728@gmail.com (M.S.); yoshihiro.hg@gmail.com (Y.H.); toshiki.kato.r8@dc.tohoku.ac.jp (T.K.); masatoshi.suzuki.c7@tohoku.ac.jp (M.S.); inabay@tohoku.ac.jp (Y.I.)
[2] Department of Radiology, Sendai Kousei Hospital, 1-20 Tsutsumidoriamamiyamachi, Aoba-ku, Sendai 981-0914, Japan; kaga@sendai-kousei-hospital.jp (Y.K.); mitsuya@sendai-kousei-hospital.jp (M.A.)
[3] Department of Radiation Disaster Medicine, International Research Institute of Disaster Science, Tohoku University, 468-1 Aramaki Aza-Aoba, Aoba-ku, Sendai 980-0845, Japan
* Correspondence: masaki.fujisawa.q1@dc.tohoku.ac.jp (M.F.); koichi.chida.d8@tohoku.ac.jp (K.C.); Tel.: +81-22-717-7943 (K.C.)

Abstract

Occupational radiation exposure in nuclear medicine presents complex spatial and temporal patterns due to the use of unsealed radiopharmaceuticals and prolonged proximity to patients. Traditional passive dosimetry provides only cumulative dose values, limiting its usefulness in identifying task-specific exposures or capturing momentary fluctuations. This study applied a real-time dosimetry system capable of second-by-second measurements, combined with time-series analysis, to evaluate staff exposure during myocardial perfusion imaging using technetium-99m. Dosimeters were placed on the left and right sides of the neck and head of two radiological technologists. Dose rates were continuously recorded throughout the injection and imaging phases. The right side of the neck received the highest cumulative and peak dose rates among all sites. Although no significant difference in total dose was observed between the injection and imaging phases, specific high-exposure events were detected. Notably, ECG lead placement and post-injection handling produced dose spikes. A positive correlation was found between administered activity and dose rate at neck-level sites but not at head-level sites. These findings demonstrate the value of real-time dosimetry in identifying procedural actions associated with elevated exposure. Time-series analysis further contextualized these peaks, supporting improved task-specific protective strategies beyond the capabilities of conventional dosimetry.

Keywords: nuclear medicine; radiation exposure; eye dose; myocardial perfusion imaging; single-photon emission computed tomography (SPECT)

Academic Editor: Thomas Lindner

Received: 4 September 2025
Revised: 9 October 2025
Accepted: 10 October 2025
Published: 14 October 2025

Citation: Fujisawa, M.; Sota, M.; Haga, Y.; Tanaka, S.; Kataoka, N.; Kato, T.; Kaga, Y.; Abe, M.; Suzuki, M.; Inaba, Y.; et al. Real-Time Monitoring of Occupational Radiation Exposure in Nuclear Medicine Technologists: An Initial Study. *Appl. Sci.* **2025**, *15*, 11008. https://doi.org/10.3390/app152011008

1. Introduction

Adverse tissue reactions resulting from radiation exposure have been well documented [1–4]. In recent years, increasing evidence has suggested the potential for stochastic effects, even at low doses [5–7]. These findings have intensified global concern over radiation protection, particularly among healthcare professionals with occupational exposure [8–10]. Consequently, more stringent regulatory standards and protective measures have been implemented, leading to reduced occupational doses across various radiological specialties [11–14].

Effective management of occupational radiation exposure is essential not only for staff safety but also for maintaining workforce well-being and public trust in radiological practices [15–17]. In clinical environments, various radiation protection measures have been introduced to reduce occupational exposure [18–22]. Comprehensive dose monitoring and targeted protective strategies are critical to minimizing the potential health risks of radiation exposure among healthcare workers, especially in high-use domains, such as nuclear medicine [23–27].

Nuclear medicine presents a unique exposure profile owing to its use of unsealed radioactive materials [28–31]. Unlike conventional radiographic procedures, where exposure is limited to brief image acquisition periods, nuclear medicine staff are continuously exposed to radiation during radiopharmaceutical preparation, injection, and patient interactions [32–34]. Ongoing advancements in radiopharmaceutical development are expected to broaden the clinical applications of nuclear medicine in both diagnostic and therapeutic settings [35,36]. Despite this prolonged exposure, lens dose protection in nuclear medicine has received comparatively little attention. The International Commission on Radiological Protection (ICRP) Publication 118 reported that lens opacities and radiation-induced cataracts may occur at lower doses than previously assumed, prompting a revision of the occupational lens dose limit to 20 mSv/year, averaged over five years [37]. In response, the International Atomic Energy Agency Technical Document (IAEA TECDOC) 1731 identified nuclear medicine as a specialty requiring specific interventions to reduce lens exposure [38]. Consequently, this issue has led to increased scrutiny of occupational eye lens exposure across many clinical disciplines in recent years [39–42]. Epidemiological studies have shown higher risks of cataracts and certain cancers among nuclear medicine personnel compared to their unexposed counterparts, emphasizing the need to improve occupational exposure assessment and control in these environments [43].

Reducing occupational exposure in nuclear medicine requires both adequate training for healthcare professionals and a clear identification of exposure-related factors [44,45]. Although passive personal dosimeters are widely used in clinical practice, they provide only cumulative dose data and cannot attribute increased exposure to specific tasks or behaviors. Consequently, there is a growing need for real-time dosimetry systems that enable second-by-second dose monitoring [46–48]. Real-time dosimetry is increasingly adopted in interventional radiology and cardiology, where it has proven useful for identifying dose peaks and informing protective behaviors [49,50]. However, its application in nuclear medicine—particularly for assessing lens exposure and task-specific contributions—remains underexplored.

Previous research has identified challenges in personal dose assessment within nuclear medicine due to spatial dose variation and frequent changes in staff positioning [51]. These findings underscore the need for a more dynamic and precise monitoring approach.

In this study, we evaluated occupational radiation exposure during nuclear medicine procedures using a real-time dosimetry system. By continuously monitoring dose rates during both the imaging and injection phases and correlating them with staff movements, we aimed to identify specific actions and time points associated with increased exposure, particularly to the neck and eye lenses. This approach offers valuable insights for enhancing shielding strategies, optimizing workflow, and implementing individualized protection measures in nuclear medicine.

2. Materials and Methods

2.1. Subjects

This study was conducted at Sendai Kosei Hospital, Japan, and involved two radiological technologists who routinely perform nuclear medicine procedures. This investigation

was designed as an exploratory pilot study to evaluate the feasibility of applying real-time dosimetry in nuclear medicine procedures. Due to the practical constraints of performing continuous second-by-second monitoring during routine clinical practice, two radiological technologists were enrolled. Both participating radiological technologists specialized in nuclear medicine practice at our institution, and all examinations were performed in accordance with applicable professional guidelines [52]. The target procedure was resting myocardial perfusion imaging using single-photon emission computed tomography (SPECT), performed with either technetium-99m methoxyisobutylisonitrile (99mTc-MIBI) or technetium-99m tetrofosmin (99mTc-tetrofosmin).

A total of 14 patients were included in the study, comprising nine radiopharmaceutical administration sessions conducted in the administration room and 13 imaging sessions performed in the SPECT room. The measurements were classified into two procedural phases: administration and imaging. The administered activity was recorded for each patient. Administered activities were measured using a CRC-55tR (Capintec, Inc., Florham Park, NJ, USA). Manufacturer specifications indicate accuracy better than ±2%, linearity within ±2%, and a response time within 2 s (4–16 s for very low-activity samples). All cases were randomly selected from routine clinical practice.

Figure 1 illustrates the procedural workflow and layouts of the administration and SPECT rooms.

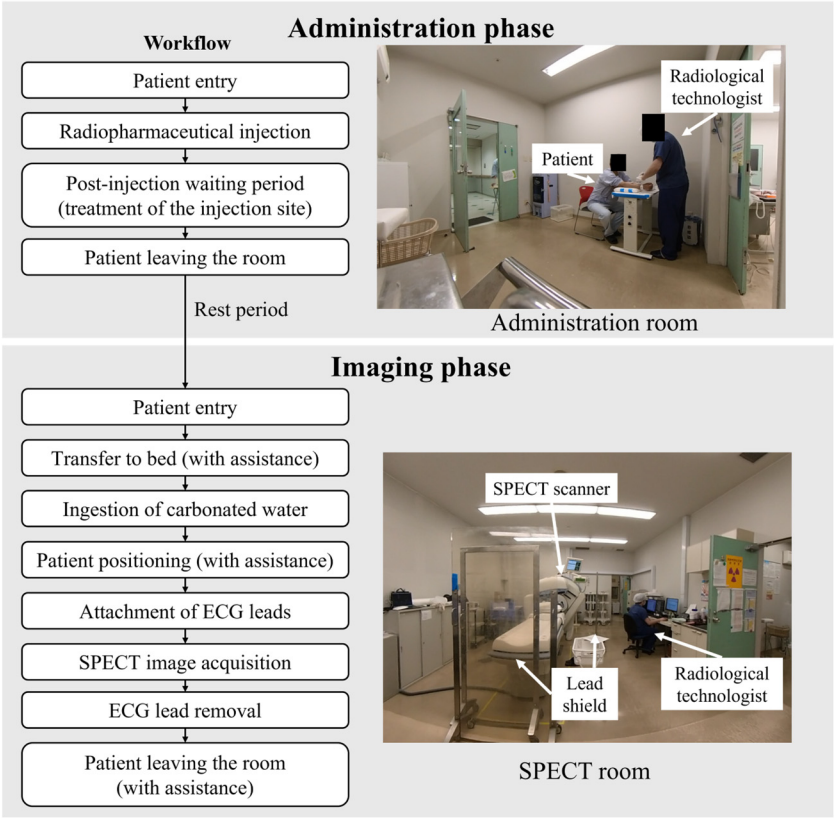

Figure 1. Workflow and room layout for myocardial perfusion SPECT procedures.

This study was approved by the ethics committee of our institution (The ethics committee of the Sendai Kosei Hospital, Approval Number: 30-19, Approved on 1 June 2021). Informed consent was obtained from all subjects.

2.2. Dosimetry

Real-time radiation monitoring was performed using the RaySafe i3 system (Unfors RaySafe AB, Billdal, Sweden). The RaySafe i3 is a semiconductor-based active personal

dosimeter and exhibits favorable baseline performance as a real-time dosimeter [53]. Within the dose rate range of 40 μSv·h^{-1} to 150 mSv·h^{-1}, the stated measurement uncertainty is the greater of 10% or 10 μSv·h^{-1} [54]. According to the manufacturer, devices undergo factory calibration (irradiation tests) during production, and conformity with specifications is verified prior to shipment. During each session, dose rate data were logged at 1 s intervals and were exported via the vendor software (Dose Viewer, version 1.3.135.0) for subsequent analysis. Dosimeters were placed on both the left and right sides of the head and neck to evaluate potential lateral differences in radiation exposure (Figure 2). In addition, simultaneous measurements at head- and neck-level allowed comparison between lens-level (head) and trunk-level (neck) exposures. This dual placement strategy provided insight into whether trunk-worn dosimeters, commonly used in clinical practice, adequately reflect actual lens dose. Using RaySafe i3, both the cumulative dose per session and the dose rate at one-second intervals were recorded. All measurements were evaluated as the 1 cm dose equivalent [Hp(10)].

Figure 2. Dosimeter placement sites on the radiological technologists.

Radiation-shielding measures were applied consistently throughout the study period following routine clinical practice. Specifically, during the radiopharmaceutical administration phase, tungsten syringe shields were used to reduce hand and body exposure. In the imaging phase, movable lead shields were strategically positioned within the examination room to further minimize ambient radiation exposure to the technologists. Additional radiation protective equipment (e.g., lead protectors) was not used in routine clinical work and was therefore not used in this study.

2.3. Data Analysis

All statistical analyses were performed using JMP Student Edition version 18.2.1 (JMP Statistical Discovery LLC, Cary, NC, USA). Statistical significance was set at $p < 0.05$. Outliers were not excluded in all analysis.

To evaluate site-specific differences in occupational radiation exposure, the cumulative dose per session was compared across four measurement positions: left head, right head, left neck, and right neck. The cumulative dose values were analyzed without distinguishing between the administration and imaging phases. Data distribution was assessed using

the Shapiro–Wilk test for normality and Levene's test for homogeneity of variance. As several variables did not satisfy these assumptions, non-parametric statistical methods were adopted. The Friedman test was used to assess overall differences among the four dosimeter positions. This test is a non-parametric repeated-measures ANOVA that analyzes rank-based data, without assuming normality or homoscedasticity. When significant differences were, post hoc pairwise comparisons were conducted using the Nemenyi test, which performs all-pairs post hoc comparisons on differences in average ranks. This procedure calculates a critical distance based on the Studentized range, thereby controlling the family-wise error rate.

To compare radiation exposure levels between procedural phases, the cumulative dose per session was analyzed separately for the administration and imaging phases at each of the four dosimeter positions. The Wilcoxon rank-sum test was used to determine whether significant differences existed between the two phases.

Linear regression analysis was performed to assess the relationship between administered radiopharmaceutical activity and cumulative radiation dose at each dosimeter site. Regression coefficients and corresponding *p*-values were calculated to evaluate the strength and significance of the correlations.

To identify specific procedural actions associated with short-term radiation exposure peaks, time-series dose rate data recorded at one-second intervals were analyzed. Using video recordings, time-series dose rate data were aligned with the corresponding workflow steps for both the administration and imaging phases. For every session, we computed the mean dose rate for each step as the sum of 1 s dose rate values divided by the corresponding detection time (Σ dose rate/detection time). Subsequently, analyses were conducted on a per-session basis to identify steps exhibiting increased dose rate and to infer plausible determinants of exposure. In accordance with the IAEA emergency preparedness guidelines, an ambient dose rate of >100 μSv/h at 1 m is used as a screening criterion to isolate potential high-exposure sources, as it indicates the possible presence of objects that could cause deterministic health effects if carried or handled [55]. Instances in which the dose rate exceeded 100 μSv/h were defined as high-exposure actions, and these moments were subsequently identified and analyzed.

3. Results

3.1. Differences by Dosimetry Position

Tables 1 and 2 summarize the cumulative doses, maximum dose rates, and administered activities recorded at each measurement site during the administration and imaging phases. The mean ± SD detection time for each phase was 52.33 ± 17.68 s in the administration phase and 57.54 ± 30.85 s in the imaging phase. Figure 3 presents a comparison of the cumulative dose per session across all measurement sites.

Table 1. Cumulative dose and administered activity during the administration phase by dosimetry positions.

Session Number	LH		RH		LN		RN		RT (A/B)	AD (MBq)
	CD (μSv)	MDR (μSv/h)	CD (μSv)	MDR (μSv/h)	CD (μSv)	MDR (μSv/h)	CD (μSv)	MDR (μSv/h)		
1	0.03	41.36	0.19	55.78	0.15	108.3	0.28	104.72	A	644.7
2	0.14	61.12	0.23	56.85	0.23	74.59	0.70	98.96	A	636.3
3	0.12	57.83	0.39	88.12	0.31	108.3	0.94	141.07	A	726.2
4	0.22	70.64	0.21	87.76	0.33	130.89	0.34	107.96	A	683.5
5	0.52	89.01	0.88	82.44	0.36	86.33	0.71	102.54	A	619.3

Table 1. *Cont.*

Session Number	LH		RH		LN		RN		RT (A/B)	AD (MBq)
	CD (μSv)	MDR (μSv/h)	CD (μSv)	MDR (μSv/h)	CD (μSv)	MDR (μSv/h)	CD (μSv)	MDR (μSv/h)		
6	0.17	59.10	0.35	74.52	0.16	61.93	0.88	114.05	A	615.4
7	0.20	94.64	0.57	79.31	0.32	76.75	0.66	186.14	A	614.2
8	0.12	87.90	0.15	78.68	0.46	102.34	1.15	125.74	B	903.9
9	0.21	64.26	0.23	71.85	0.50	108.00	1.28	134.34	B	862.3
Mean	0.19		0.35		0.31		0.77			700.64
SD	0.13		0.22		0.12		0.32			103.83

LH, left head; RH, right head; LN, left neck; RN, right neck; RT, radiological technologist; AD, administered activity; CD, cumulative dose; MDR, maximum dose rate. Uncertainties: Approximate measurement uncertainties were ±2% for the administered activity and ±10 μSv/h (or 10%) for the maximum dose rate.

Table 2. Cumulative dose and administered activity during the imaging phase by dosimetry positions.

Session Number	LH		RH		LN		RN		RT (A/B)	AD (MBq)
	CD (μSv)	MDR (μSv/h)	CD (μSv)	MDR (μSv/h)	CD (μSv)	MDR (μSv/h)	CD (μSv)	MDR (μSv/h)		
1	0.22	56.14	0.41	79.66	0.60	114.43	0.91	133.72	A	731.9
2	0.21	76.11	0.33	106.45	0.22	58.11	0.80	136.95	A	486.7
3	0.17	52.86	0.19	97.66	0.20	69.53	0.46	141.85	A	944.5
4	0.22	54.35	0.25	78.62	0.20	64.94	0.50	137.90	A	691.8
5	0.17	74.82	0.25	81.09	0.03	34.24	0.37	96.96	A	639.3
6	0.36	107.65	0.27	96.62	0.44	63.30	0.55	153.80	A	644.7
7	0.15	100.42	0.26	85.92	0.28	77.96	0.21	134.94	A	636.3
8	0.28	62.85	0.35	60.85	0.46	72.24	0.63	145.09	A	683.5
9	0.48	82.05	0.63	99.94	0.28	74.25	0.44	119.58	A	619.3
10	0.35	107.59	0.40	83.22	0.38	112.00	0.40	92.89	A	615.4
11	0.25	66.99	0.55	81.09	0.30	107.90	0.77	150.30	A	614.2
12	0.07	41.71	0.06	51.80	0.69	104.51	3.23	185.17	B	903.9
13	0.11	56.10	0.38	80.12	0.77	88.96	1.04	135.00	B	862.3
Mean	0.23		0.33		0.37		0.79			697.98
SD	0.10		0.14		0.20		0.71			121.40

LH, left head; RH, right head; LN, left neck; RN, right neck; RT, radiological technologist; AD, administered activity; CD, cumulative dose; MDR, maximum dose rate. Uncertainties: Approximate measurement uncertainties were ±2% for the administered activity and ±10 μSv/h (or 10%) for the maximum dose rate.

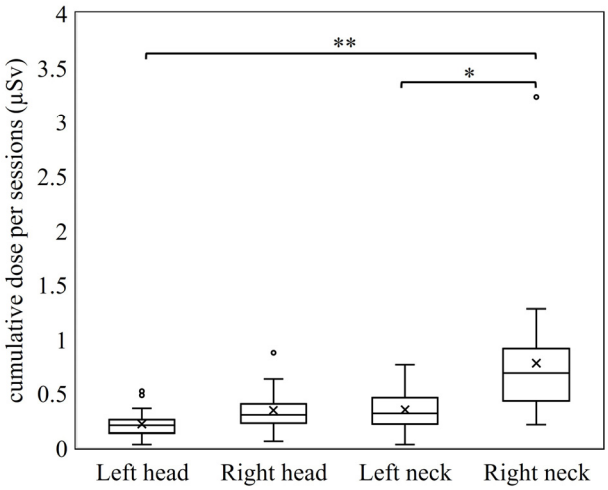

Figure 3. Cumulative dose per session at each dosimeter position. * $p < 0.05$, ** $p < 0.001$.

The Friedman test revealed statistically significant differences among the two measurement sites. Post hoc Nemenyi tests identified significant differences between the following pairs: right and left neck, right neck and right head, right neck and left head, and left and right head. Among all sites, the right neck exhibited the highest cumulative dose and tended to show the highest peak dose rates.

3.2. Comparison of Radiation Exposure Between the Administration and Imaging Phases

Figure 4 shows the cumulative dose per session at each dosimeter position during the radiopharmaceutical administration and imaging phases. No statistically significant differences in cumulative dose were observed between the two phases at any of the four measurement sites. Although the median dose at the neck positions was slightly higher during the administration phase, this difference was not statistically significant.

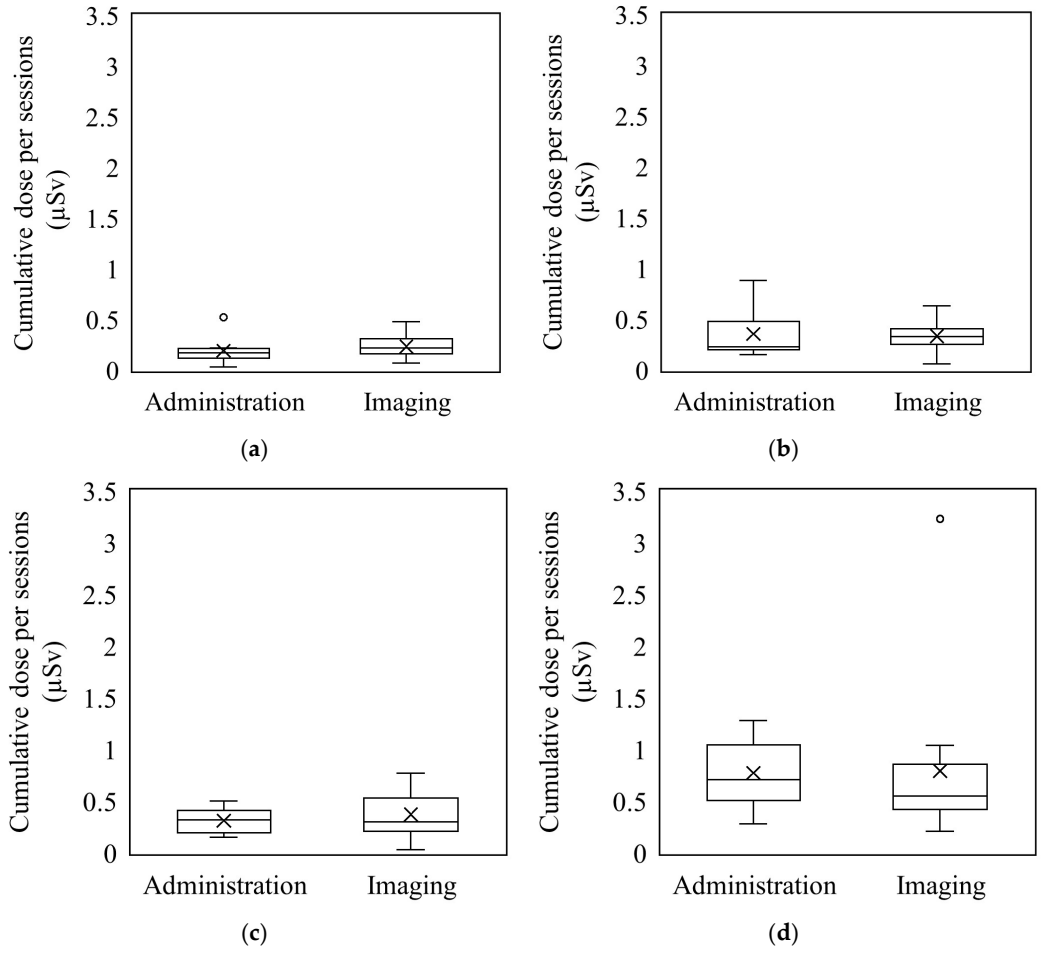

Figure 4. Cumulative dose per session during the administration and imaging phases: (**a**) left head, (**b**) right head, (**c**) left neck, (**d**) right neck.

3.3. Relationship Between Administered Activity and Exposure

Figure 5 illustrates the relationship between administered activity and cumulative dose per session at each dosimeter position. At the neck (left/right), there appears to be a slight tendency toward higher dose with higher activity, whereas the head positions show a possible inverse tendency. However, explained variance is low (low R^2); these patterns should be regarded as suggestive rather than definitive.

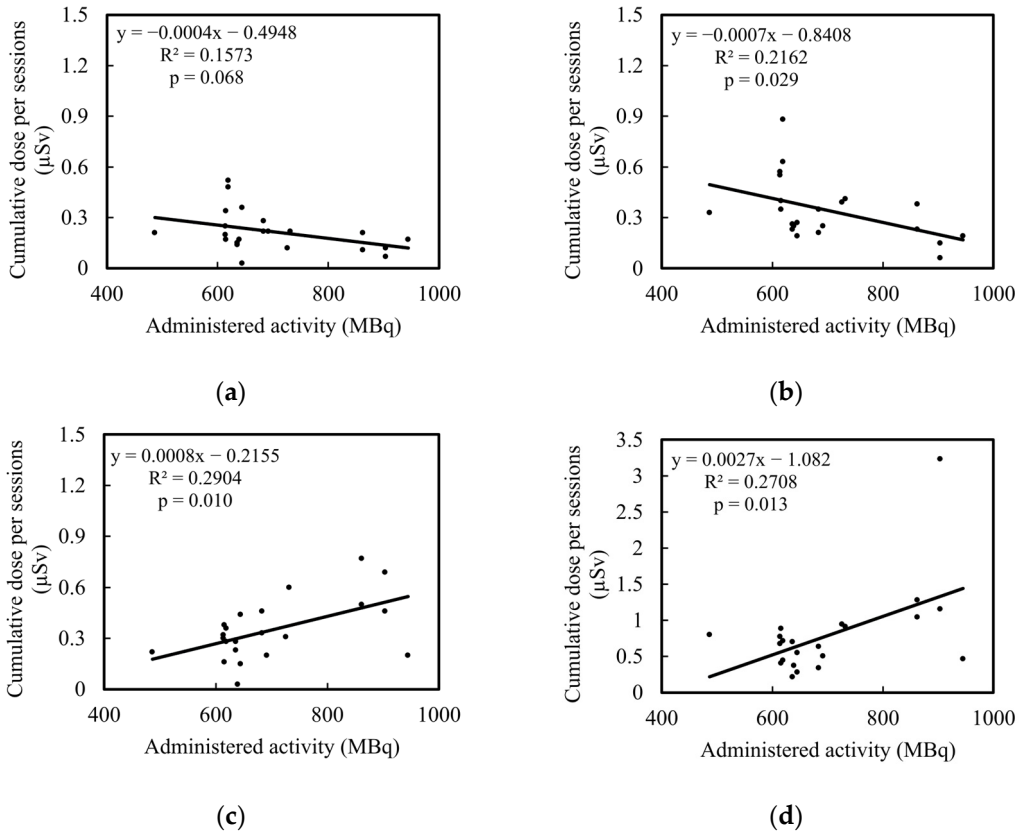

Figure 5. Correlation between administered activity and cumulative dose at each measurement site: (**a**) left head, (**b**) right head, (**c**) left neck, (**d**) right neck.

3.4. Identification of Exposure-Causing Actions

To identify specific tasks contributing to radiation exposure, time-series dose rate data were analyzed at one-second intervals for each measurement site. Figures 6 and 7 summarize the mean dose rate for each workflow step during the administration and imaging phases, respectively. In the administration phase, a pronounced increase in dose rate was observed during the injection step. In the imaging phase, elevated mean dose rates were noted during patient positioning immediately before and after SPECT acquisition and during electrocardiogram (ECG) lead placement/removal.

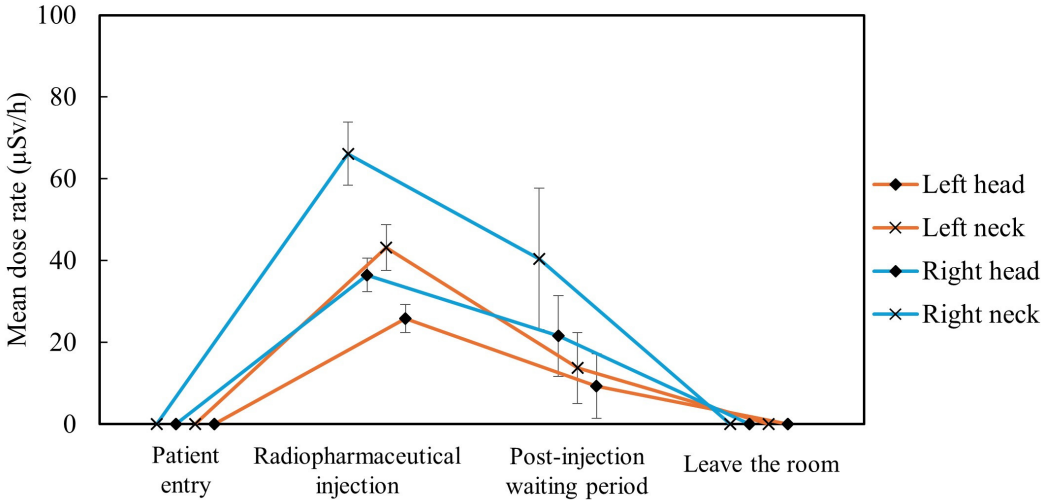

Figure 6. Mean dose rate by workflow step during the administration phase. Error bars indicate 95% confidence intervals across sessions.

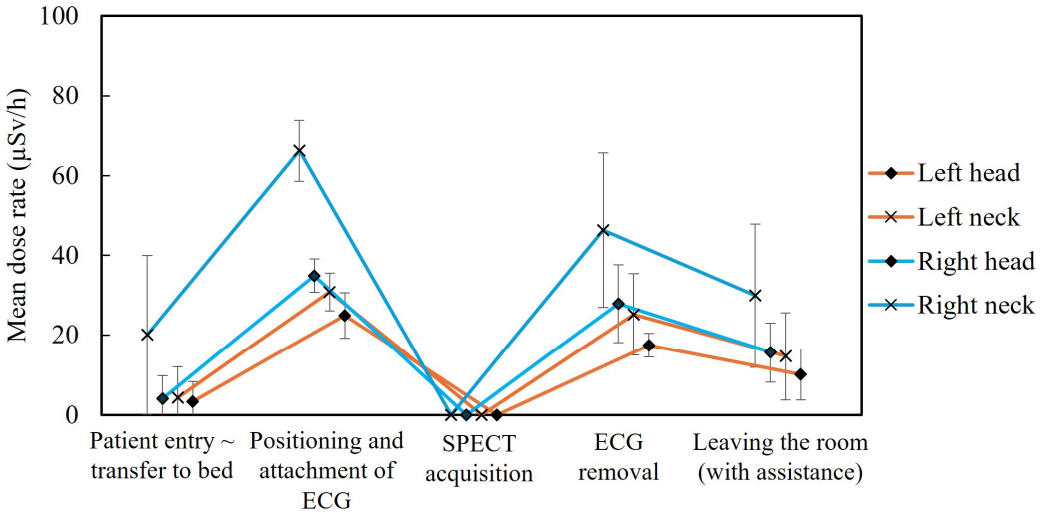

Figure 7. Mean dose rate by workflow step during the imaging phase. Error bars indicate 95% confidence intervals across sessions.

Figures 8 and 9 depict the sessions with the highest recorded peak dose rates during the administration and imaging phases, respectively. In the administration phase (Figure 8), no measurable radiation was detected before the radiopharmaceutical injection. A sharp increase in dose rate—often exceeding 100 μSv/h—was consistently observed immediately after injection. Smaller peaks also occurred during post-injection handling, such as treatment of the injection site.

In the imaging phase (Figure 9), dose rate peaks—often exceeding 100 μSv/h—were most frequently recorded during electrocardiogram (ECG) lead placement and removal. Additional peaks were observed during tasks requiring close patient assistance, such as bed transfer and patient positioning, which involved proximity to the patient's thoracoabdominal region. In contrast, no measurable radiation was detected during the SPECT image acquisition.

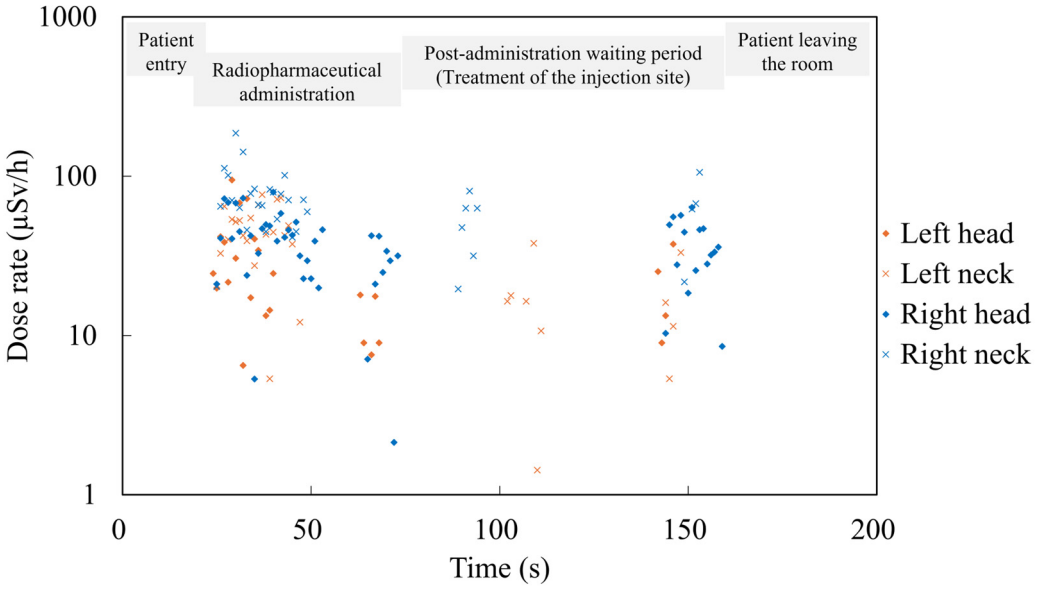

Figure 8. Time-series dose rate data during an administration session with the highest peak. A sharp increase was observed immediately after injection, with additional smaller peaks during post-injection handling.

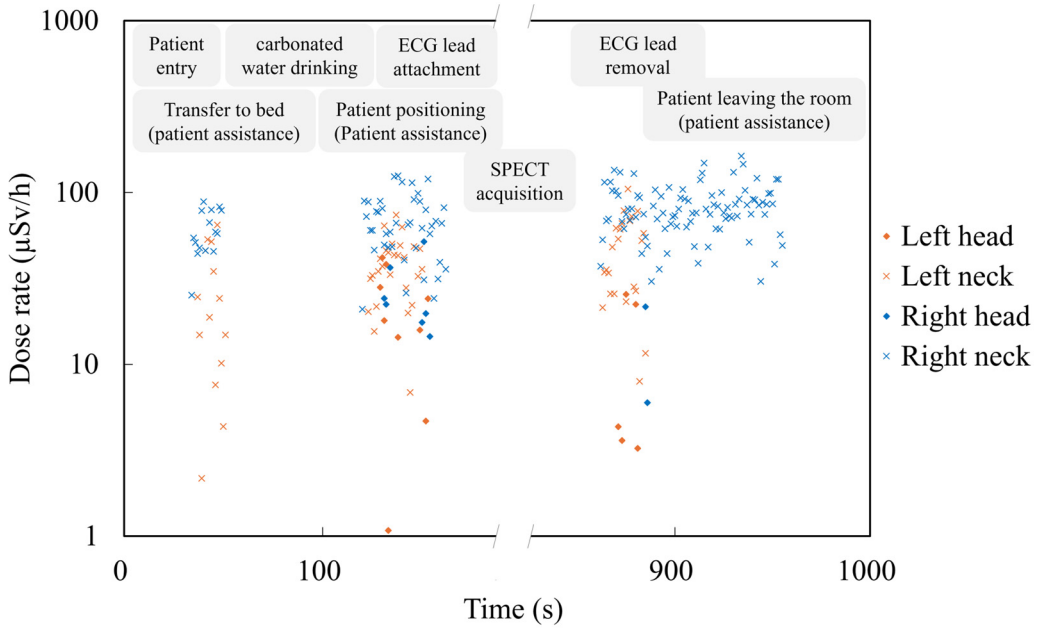

Figure 9. Time-series dose rate data during an imaging session with the highest peak. Peaks occurred mainly during ECG lead placement and removal, while no measurable radiation was detected during SPECT acquisition.

4. Discussion

Radiation dose management is a critical concern across medical disciplines [56], including diagnostic radiology [57,58], interventional cardiology [59–61], and radiation therapy [62,63]. In nuclear medicine, where staff are exposed to gamma photons emitted from unsealed radiopharmaceuticals, the energy characteristics differ significantly. Gamma radiation has higher photon energy and deeper tissue penetration, rendering conventional protective strategies less effective. Therefore, nuclear medicine requires different radiation protection approaches, often involving alternative materials, shielding configurations, or workflow designs tailored to its unique exposure conditions.

In this study, we employed a real-time dosimetry system capable of recording dose rates on a second-by-second basis throughout nuclear medicine procedures. Unlike passive dosimeters, which yield only cumulative retrospective data, real-time systems capture the timing and context of specific tasks or movements associated with elevated exposure. In the absence of real-time lens dosimeters at present, we have evaluated near-eye exposure patterns using this device. This approach enables a more nuanced understanding of occupational doses and supports the development of targeted safety interventions.

Our findings revealed significant variations in dose depending on the anatomical site of measurement. The right neck consistently exhibited the highest cumulative and peak doses, likely influenced by the technologists' handedness, body orientation, and procedural habits. These results indicate that individual working styles and laterality can produce substantial asymmetry in exposure levels between the left and right sides of the body. Notably, cumulative doses at head positions remained below 2 μSv across both the administration and imaging phases combined. Given these findings, it is unlikely that technologists performing nuclear medicine procedures would exceed the annual eye lens dose limit of 20 mSv or the ICRP threshold of 0.5 Gy over 5 years. However, this does not necessarily guarantee an accurate assessment of eye lens exposure. Dose estimates based solely on trunk-mounted personal dosimeters may not fully reflect the actual dose received by the eye lens. Therefore, careful interpretation of dose measurements is warranted, particularly in clinical environments with complex spatial exposure patterns.

Although cumulative doses did not differ significantly between the administration and imaging phases overall, some imaging sessions were associated with higher exposures. These cases typically involved patients requiring additional assistance owing to their poor physical condition, resulting in prolonged close contact between staff and the radiation source.

Analysis of the relationship between administered activity and radiation dose suggested a weak positive tendency at the neck positions and a possible inverse tendency at the head-level sites, with low R^2 indicating limited explanatory power. The neck correlation is expected, as this region is more frequently exposed during close-contact procedures and typically lacks substantial shielding. In contrast, the negative correlation observed at the head positions is likely incidental, possibly due to low-dose levels or variability in positioning.

During injection procedures, technologists generally maintained a greater distance from patients, especially at the head level, which likely contributed to reduced lens-region exposure. Dose rate spikes during the injection phase were brief and typically occurred immediately after radiopharmaceutical administration. The use of tungsten syringe shielding effectively mitigated these peaks, reaffirming the importance of shielding practices and proper user training.

The most prominent dose rate peaks during imaging were observed during the placement and removal of ECG leads. These tasks require staff members to work in close proximity to the patient's upper abdomen and thoracic region. It is well-established that approximately one hour after administration, 99mTc-MIBI accumulates most intensely in the liver [64]. Previous studies have also shown that among various measurement positions around the patient (head, chest, and foot), the chest region consistently yields the highest occupational exposure [65]. Although close patient contact during ECG lead handling is often unavoidable, our findings underscore the need to provide staff with feedback regarding the elevated radiation exposure associated with this specific task. In contrast, no measurable radiation dose was detected during imaging acquisition itself, likely owing to the increased distance (~2 m) between staff and patient and the use of lead shielding barriers. These observations emphasize how procedural planning and physical layout can directly influence occupational dose levels.

While this study focused specifically on myocardial perfusion imaging using 99mTc, the exposure patterns observed may be relevant to other nuclear medicine procedures. However, further investigations across various radiopharmaceuticals and clinical workflows are necessary to validate the generalizability of our findings.

This study had certain limitations. The sample size was small, and the analysis was limited to a single procedure type and radiopharmaceutical at a single institution. These factors may limit the generalizability of the findings and should be considered when interpreting the results. Nevertheless, these participants performed routine procedures representative of daily clinical practice, and the exposure patterns observed—such as elevated doses during radiopharmaceutical injection and ECG lead handling—are consistent with tasks universally performed in nuclear medicine. Thus, while the present results should be interpreted as preliminary, they provide important pilot data that can guide the design of larger-scale studies in the future. In addition, the dosimeter used in this study specifies a measurement uncertainty of the greater of $\pm 10\%$ or ± 10 μSv/h. Therefore, small differences or subtle trends at low dose rates should be interpreted with caution. As the dosimeter was not designed for eye-lens dosimetry, precise lens dose Hp(3) cannot be obtained. Results should be regarded as near-eye exposure trends, not direct lens-dose estimates.

Future studies should expand real-time dosimetry to include extremity dose monitoring and examine a broader range of nuclear medicine procedures and isotopes. Real-time monitoring can provide actionable feedback on task-specific exposure patterns and support the development of evidence-based, procedure-tailored radiation protection strategies in nuclear medicine.

5. Conclusions

This study employed real-time dosimetry with one-second interval measurements to evaluate occupational radiation exposure during nuclear medicine procedures, offering novel insights through time-series dose rate analysis. Our findings demonstrated that the right neck received significantly higher radiation doses than other anatomical sites, underscoring the limitations of conventional dosimeter placement. Although no significant overall dose differences were observed between the imaging and injection phases, higher exposures were occasionally recorded during imaging sessions requiring additional patient assistance. The highest peak dose rates occurred during ECG lead placement and removal, identifying these tasks as key contributors to staff exposure due to close contact with the patient's thoracic region. Maintaining appropriate distance from patients and using protective equipment such as tungsten syringe shields proved effective in minimizing exposure. These results support the integration of real-time dosimetry into routine clinical workflows. By enabling task-specific exposure assessments, real-time systems can guide the development of optimized shielding protocols, improved procedural designs, and personalized radiation protection measures for nuclear medicine personnel.

Author Contributions: Conceptualization, Y.H., Y.K., M.A., and K.C.; methodology, M.S. (Masahiro Sota), Y.H., and K.C.; software, M.F., M.S. (Masahiro Sota), M.S. (Masatoshi Suzuki), and Y.I.; validation, M.F., M.S. (Masahiro Sota), Y.H., S.T., N.K., M.S. (Masatoshi Suzuki), Y.I. and K.C.; formal analysis, M.F., M.S. (Masahiro Sota), Y.H., and T.K.; investigation, M.F., M.S. (Masahiro Sota), Y.H., S.T., N.K., T.K., Y.K., and M.A.; resources, Y.K., M.A., and K.C.; data curation, M.F., M.S. (Masahiro Sota), Y.H., M.S. (Masatoshi Suzuki), and Y.I.; writing—original draft preparation, M.F.; writing—review and editing, Y.H., M.S. (Masatoshi Suzuki), Y.I., and K.C.; visualization, M.F., S.T., N.K., and T.K.; supervision, Y.K., M.A., and K.C.; project administration, Y.H., and K.C.; funding acquisition, M.F., and K.C. All authors have read and agreed to the published version of the manuscript.

Funding: This work was supported in part by the Industrial Disease Clinical Research Grants (Grant Number 240401-02), the program of NRA Human Resource Development, Human Resource Development Program for Advanced Radiation Protection with Practical Problem-Solving Skills, Japan, and JST SPRING (Grant Number JPMJSP2114).

Institutional Review Board Statement: This study was conducted in accordance with the Declaration of Helsinki, and the protocol was approved by the Ethics Committee of Sendai Kousei Hospital, Japan (approval number; 30-19) on 1 June 2021.

Informed Consent Statement: Informed consent for participation was obtained from all subjects involved in this study.

Data Availability Statement: The data presented in this study are available on request from the corresponding author due to privacy and ethical restrictions.

Acknowledgments: We thank Kodai Sagehashi and Ryota Shindo from Tohoku University Graduate School of Medicine, and Saki Takahira from Sendai Kosei Hospital for their invaluable assistance.

Conflicts of Interest: The authors declare no conflicts of interest.

Abbreviations

The following abbreviations are used in this manuscript:

ECG	Electrocardiogram
IAEA	International Atomic Energy Agency
ICRP	International Commission on Radiological Protection
MIBI	Methoxyisobutylisonitrile
SPECT	Single-Photon Emission Computed Tomography

References

1. Rajaraman, P.; Doody, M.M.; Yu, C.L.; Preston, D.L.; Miller, J.S.; Sigurdson, A.J.; Freedman, D.M.; Alexander, B.H.; Little, M.P.; Miller, D.L.; et al. JOURNAL CLUB: Cancer Risks in U.S. Radiologic Technologists Working with Fluoroscopically Guided Interventional Procedures, 1994–2008. *Am. J. Roentgenol.* **2016**, *206*, 1101–1109. [CrossRef] [PubMed]
2. Su, Y.; Wang, Y.; Yoshinaga, S.; Zhu, W.; Tokonami, S.; Zou, J.; Tan, G.; Tsuji, M.; Akiba, S.; Sun, Q. Lens Opacity Prevalence among the Residents in High Natural Background Radiation Area in Yangjiang, China. *J. Radiat. Res.* **2021**, *62*, 67–72. [CrossRef] [PubMed]
3. Little, M.P.; Cahoon, E.K.; Kitahara, C.M.; Simon, S.L.; Hamada, N.; Linet, M.S. Occupational Radiation Exposure and Excess Additive Risk of Cataract Incidence in a Cohort of US Radiologic Technologists. *Occup. Environ. Med.* **2020**, *77*, 1–8. [CrossRef] [PubMed]
4. Hijikata, Y.; Yamashita, K.; Hatsusaka, N.; Nagata, T.; Kitamura, H.; Morota, K.; Matsuzaki, S.; Nakagami, K.; Hitomi, G.; Kuriyama, T.; et al. Prevalence of Cataractous Changes in the Eyes and Chronic Inflammatory Changes in the Hands Among Spine Surgeons. *J. Bone Jt. Surg.* **2025**, *107*, e25. [CrossRef]
5. Preston, D.L.; Kitahara, C.M.; Freedman, D.M.; Sigurdson, A.J.; Simon, S.L.; Little, M.P.; Cahoon, E.K.; Rajaraman, P.; Miller, J.S.; Alexander, B.H.; et al. Breast Cancer Risk and Protracted Low-to-Moderate Dose Occupational Radiation Exposure in the US Radiologic Technologists Cohort, 1983–2008. *Br. J. Cancer* **2016**, *115*, 1105–1112. [CrossRef]
6. Kitahara, C.M.; Linet, M.S.; Drozdovitch, V.; Alexander, B.H.; Preston, D.L.; Simon, S.L.; Freedman, D.M.; Brill, A.B.; Miller, J.S.; Little, M.P.; et al. Cancer and Circulatory Disease Risks in US Radiologic Technologists Associated with Performing Procedures Involving Radionuclides. *Occup. Environ. Med.* **2015**, *72*, 770–776. [CrossRef]
7. Berrington de Gonzalez, A.; Daniels, R.D.; Cardis, E.; Cullings, H.M.; Gilbert, E.; Hauptmann, M.; Kendall, G.; Laurier, D.; Linet, M.S.; Little, M.P.; et al. Epidemiological Studies of Low-Dose Ionizing Radiation and Cancer: Rationale and Framework for the Monograph and Overview of Eligible Studies. *J. Natl. Cancer Inst. Monogr.* **2020**, *2020*, 97–113. [CrossRef]
8. International Commission on Radiological Protection (ICRP). *Avoidance of Radiation Injuries from Medical Interventional Procedures*; ICRP Publication 85; ICRP: Pergamon, Turkey; Oxford, UK, 2000; Volume 30.
9. International Commission on Radiological Protection (ICRP). Radiation dose to patients from radiopharmaceuticals: A compendium of current information related to frequently used substances. ICRP Publication 128. *Ann. ICRP* **2015**, *47*, 7–321.
10. Forbrig, R.; Trumm, C.G.; Reidler, P.; Kunz, W.G.; Dimitriadis, K.; Kellert, L.; Rückel, J.; Liebig, T.; Stahl, R. Optimizing Radiation Dose and Image Quality in Stroke CT Protocols: Proposed Diagnostic Reference Levels for Multiphase CT Angiography and Perfusion Imaging. *Diagnostics* **2024**, *14*, 2866. [CrossRef]
11. Yoshinaga, S.; Mabuchi, K.; Sigurdson, A.J.; Doody, M.M.; Ron, E. Cancer Risks among Radiologists and Radiologic Technologists: Review of Epidemiologic Studies. *Radiology* **2004**, *233*, 313–321. [CrossRef]
12. Boice, J., Jr.; Dauer, L.T.; Kase, K.R.; Mettler, F.A., Jr.; Vetter, R.J. Evolution of Radiation Protection for Medical Workers. *Br. J. Radiol.* **2020**, *93*, 20200282. [CrossRef] [PubMed]
13. Linet, M.S.; Kim, K.P.; Miller, D.L.; Kleinerman, R.A.; Simon, S.L.; de Gonzalez, A.B. Historical Review of Occupational Exposures and Cancer Risks in Medical Radiation Workers. *Radiat. Res.* **2010**, *174*, 793–808. [CrossRef]
14. Endo, M.; Haga, Y.; Sota, M.; Tanaka, A.; Otomo, K.; Murabayashi, Y.; Abe, M.; Kaga, Y.; Inaba, Y.; Suzuki, M.; et al. Evaluation of Novel X-Ray Protective Eyewear in Reducing the Eye Dose to Interventional Radiology Physicians. *J. Radiat. Res.* **2021**, *62*, 414–419. [CrossRef]
15. International Commission on Radiological Protection (ICRP). Occupational radiological protection in interventional procedures. ICRP Publication 139. *Ann. ICRP* **2018**, *47*, 1–118. [CrossRef]
16. International Atomic Energy Agency (IAEA). *Occupational Radiation Protection: General Safety Guide*; IAEA Safety Standards Series No. GSG-7; IAEA: Vienna, Austria, 2018; pp. 1–152.
17. International Atomic Energy Agency (IAEA). *Radiation Protection and Safety of Radiation Sources: International Basic Safety Standards*; IAEA Safety Standards Series No. GSR Part 3; IAEA: Vienna, Austria, 2014; pp. 1–436.

18. Shindo, R.; Ohno, S.; Yamamoto, K.; Konta, S.; Inaba, Y.; Suzuki, M.; Zuguchi, M.; Chida, K. Comparison of Shielding Effects of Over-Glasses-Type and Regular Eyewear in Terms of Occupational Eye Dose Reduction. *J. Radiol. Prot.* **2024**, *44*, 023501. [CrossRef]
19. Kato, M.; Chida, K.; Munehisa, M.; Sato, T.; Inaba, Y.; Suzuki, M.; Zuguchi, M. Non-Lead Protective Aprons for the Protection of Interventional Radiology Physicians from Radiation Exposure in Clinical Settings: An Initial Study. *Diagnostics* **2021**, *11*, 1613. [CrossRef]
20. McVey, S.; Sandison, A.; Sutton, D.G. An Assessment of Lead Eyewear in Interventional Radiology. *J. Radiol. Prot.* **2013**, *33*, 647. [CrossRef]
21. Fujisawa, M.; Haga, Y.; Takahira, S.; Sota, M.; Kato, T.; Abe, M.; Kaga, Y.; Inaba, Y.; Suzuki, M.; Chida, K. Development of a Headgear-Based Eye Protection Device for Physicians Performing Fluoroscopy-Guided Bronchoscopy. *J. Radiat. Res.* **2025**, *66*, 372–384. [CrossRef]
22. Lin, H.-H.; Lai, L.-H.; Tang, K.-T.; Ting, C.-Y.; Lai, C.-S. Radiation Dose Assessment of the Fog Lead Acrylic Shields during Coronary Angiography: A Phantom Study. *Appl. Sci.* **2021**, *11*, 10743. [CrossRef]
23. Lindholm, C.; Pekkarinen, A.; Sipilä, O.; Manninen, A.-L.; Lehtinen, M.; Siiskonen, T. Estimation of Hp(3) among Staff Members in Two Nuclear Medicine Units in Finland. *Radiat. Prot. Dosim.* **2020**, *190*, 176–184. [CrossRef] [PubMed]
24. Guiu-Souto, J.; Sánchez-García, M.; Vázquez-Vázquez, R.; Otero, C.; Luna, V.; Mosquera, J.; Busto, R.L.; Aguiar, P.; Ruibal, Á.; Pardo-Montero, J.; et al. Evaluation and Optimization of Occupational Eye Lens Dosimetry during Positron Emission Tomography (PET) Procedures. *J. Radiol. Prot.* **2016**, *36*, 299. [CrossRef]
25. Krajewska, G.; Krajewski, P. Evaluation of Internal Exposure of Nuclear Medicine Staff Working with Radioiodine in Poland. *Int. J. Occup. Med. Environ. Health* **2023**, *36*, 587–595. [CrossRef]
26. Struelens, L.; Aalbersberg, E.; Beels, L.; Cherbuin, N.; D'Asseler, Y.; De Monte, F.; Lopez Medina, A.; del Carmen Riveira Martin, M.; Schoonjans, W.; Terwinghe, C.; et al. How Much Do 68Ga-, 177Lu- and 131I-Based Radiopharmaceuticals Contribute to the Global Radiation Exposure of Nuclear Medicine Staff? *EJNMMI Phys.* **2024**, *11*, 95. [CrossRef] [PubMed]
27. Mettler, F.A.; Guiberteau, M.J. Occupational Exposure in General Radiology and Nuclear Medicine: A Changing Target. *Radiology* **2021**, *300*, 613–614. [CrossRef]
28. Villoing, D.; Yoder, R.C.; Passmore, C.; Bernier, M.-O.; Kitahara, C.M. A U.S. Multicenter Study of Recorded Occupational Radiation Badge Doses in Nuclear Medicine. *Radiology* **2018**, *287*, 676–682. [CrossRef]
29. Villoing, D.; Borrego, D.; Preston, D.L.; Alexander, B.H.; Rose, A.; Salasky, M.; Linet, M.S.; Lee, C.; Kitahara, C.M. Trends in Occupational Radiation Doses for U.S. Radiologic Technologists Performing General Radiologic and Nuclear Medicine Procedures, 1980–2015. *Radiology* **2021**, *300*, 605–612. [CrossRef] [PubMed]
30. Marshall, S.K.; Sirieak, N.; Karnkorn, P.; Keawtong, V.; Hayeeabdunromae, A.; Noomad, N.; Durawee, W.; Cheewakul, J. Nuclear Medicine Radiological Hot Laboratory Simulation: A Mixed-Method Intervention Study on Immersive Virtual Reality for Sustainable Education. *Appl. Sci.* **2024**, *14*, 5041. [CrossRef]
31. Marshall, S.K.; Hayeeabdunromae, A.; Noomad, N.; Durawee, W.; Sirieak, N.; Karnkorn, P.; Keawtong, V. Evaluation of Environmental Radiation Exposure and Algorithms for Determining the Occupational Effective Dose During 99mTc-MDP Bone Scintigraphy: A Comprehensive Analysis. *Appl. Sci.* **2024**, *14*, 11211. [CrossRef]
32. Wrzesień, M.; Królicki, L.; Albiniak, Ł.; Olszewski, J. Is Eye Lens Dosimetry Needed in Nuclear Medicine? *J. Radiol. Prot.* **2018**, *38*, 763. [CrossRef]
33. Wrzesień, M.; Albiniak, Ł. Personal Dose Equivalent Hp(0.07) during 68Ga-DOTA-TATE Production Procedures. *Radiat. Environ. Biophys.* **2023**, *62*, 117–129. [CrossRef] [PubMed]
34. Marshall, S.K.; Prom-on, P.; Sangkue, S.; Thiangsook, W. Assessment of Radiation Exposure in a Nuclear Medicine Department during 99mTc-MDP Bone Scintigraphy. *Toxics* **2023**, *11*, 814. [CrossRef]
35. Mettler, F.A.; Bhargavan, M.; Faulkner, K.; Gilley, D.B.; Gray, J.E.; Ibbott, G.S.; Lipoti, J.A.; Mahesh, M.; McCrohan, J.L.; Stabin, M.G.; et al. Radiologic and Nuclear Medicine Studies in the United States and Worldwide: Frequency, Radiation Dose, and Comparison with Other Radiation Sources—1950–2007. *Radiology* **2009**, *253*, 520–531. [CrossRef]
36. Slomka, P.J.; Pan, T.; Berman, D.S.; Germano, G. Advances in SPECT and PET Hardware. *Prog. Cardiovasc. Dis.* **2015**, *57*, 566–578. [CrossRef] [PubMed]
37. Stewart, F.A.; Akleyev, A.V.; Hauer-Jensen, M.; Hendry, J.H.; Kleiman, N.J.; Macvittie, T.J.; Aleman, B.M.; Edgar, A.B.; Mabuchi, K.; Muirhead, C.R. ICRP Publication 118: ICRP Statement on Tissue Reactions and Early and Late Effects of Radiation in Normal Tissues and Organs–Threshold Doses for Tissue Reactions in a Radiation Protection Context. *Ann. ICRP* **2012**, *41*, 1–322. [CrossRef]
38. International Atomic Energy Agency (IAEA). *Implications for Occupational Radiation Protection of the New Dose Limit for the Lens of the Eye*; IAEA: Vienna, Austria, 2013; Volume 1731, pp. 1–34.
39. Yamada, A.; Haga, Y.; Sota, M.; Abe, M.; Kaga, Y.; Inaba, Y.; Suzuki, M.; Tada, N.; Zuguchi, M.; Chida, K. Eye Lens Radiation Dose to Nurses during Cardiac Interventional Radiology: An Initial Study. *Diagnostics* **2023**, *13*, 3003. [CrossRef]

40. Ohno, S.; Konta, S.; Shindo, R.; Yamamoto, K.; Isobe, R.; Inaba, Y.; Suzuki, M.; Zuguchi, M.; Chida, K. Effect of Backscatter Radiation on the Occupational Eye-Lens Dose. *J. Radiat. Res.* **2024**, *65*, 450–458. [CrossRef] [PubMed]
41. Osanai, M.; Sato, H.; Sato, K.; Kudo, K.; Hosoda, M.; Hosokawa, S.; Kitajima, M.; Tsushima, M.; Fujita, A.; Hosokawa, Y.; et al. Occupational Radiation Dose, Especially for Eye Lens: Hp(3), in Medical Staff Members Involved in Computed Tomography Examinations. *Appl. Sci.* **2021**, *11*, 4448. [CrossRef]
42. Inaba, Y.; Hitachi, S.; Watanuki, M.; Chida, K. Occupational Radiation Dose to Eye Lenses in CT-Guided Interventions Using MDCT-Fluoroscopy. *Diagnostics* **2021**, *11*, 646. [CrossRef]
43. Bernier, M.-O.; Journy, N.; Villoing, D.; Doody, M.M.; Alexander, B.H.; Linet, M.S.; Kitahara, C.M. Cataract Risk in a Cohort of U.S. Radiologic Technologists Performing Nuclear Medicine Procedures. *Radiology* **2018**, *286*, 592–601. [CrossRef]
44. Vañó, E.; Rosenstein, M.; Liniecki, J.; Rehani, M.M.; Martin, C.J.; Vetter, R.J. ICRP Publication 113. Education and Training in Radiological Protection for Diagnostic and Interventional Procedures. *Ann. ICRP* **2009**, *39*, 7–68. [CrossRef]
45. Cousins, C.; Miller, D.L.; Bernardi, G.; Rehani, M.M.; Schofield, P.; Vañó, E.; Einstein, A.J.; Geiger, B.; Heintz, P.; Padovani, R.; et al. ICRP Publication 120: Radiological Protection in Cardiology. *Ann. ICRP* **2013**, *42*, 1–125. [CrossRef] [PubMed]
46. Apostolou, A.; Leichert, H.J.; König, A.M.; Owczarek, A.D.; Mahnken, A.H. Efficiency in Radiation Protection of a Novel Exoskeleton-Based Interventional Radiology Apron and Correlation with Conventional Aprons. *Eur. J. Radiol.* **2025**, *184*, 111946. [CrossRef]
47. Crowhurst, J.A.; Tse, J.; Mirjalili, N.; Savage, M.L.; Raffel, O.C.; Gaikwad, N.; Walters, D.L.; Dautov, R. Trial of a Novel Radiation Shielding Device to Protect Staff in the Cardiac Catheter Laboratory. *Am. J. Cardiol.* **2023**, *203*, 429–435. [CrossRef]
48. Lundvall, L.-L.; Sandborg, M. Does Radiological Protection Training or a Real-Time Staff Dosemeter Display Reduce Staff Doses During X-Ray-Guided Pulmonary Bronchoscopy? *Radiat. Prot. Dosim.* **2022**, *198*, 265–273. [CrossRef] [PubMed]
49. Casazza, R.; Malik, B.; Hashmi, A.; Fogel, J.; Montagna, E.; Gibson, D.; Palacio, A.; Beginyazova, H.; Frankel, R.; Shani, J. The Influence of Height on Occupational Radiation Exposure of Interventional Cardiologists During Selective Coronary Angiography Using a Radial Artery Approach. *Am. J. Cardiol.* **2025**, *251*, 1–8. [CrossRef]
50. Casazza, R.; Malik, B.; Hashmi, A.; Fogel, J.; Montagna, E.; Frankel, R.; Borgen, E.; Ayzenberg, S.; Friedman, M.; Moskovits, N.; et al. Operator Radiation Exposure Comparing the Left Radial Artery Approach and a Uniform Hyper-Adducted Right Radial Artery Approach: The HARRA Study. *Circ.-Cardiovasc. Interv.* **2025**, *18*, e014602. [CrossRef] [PubMed]
51. Fujisawa, M.; Haga, Y.; Sota, M.; Abe, M.; Kaga, Y.; Inaba, Y.; Suzuki, M.; Meguro, T.; Hosoi, Y.; Chida, K. Evaluation of Lens Doses among Medical Staff Involved in Nuclear Medicine: Current Eye Radiation Exposure among Nuclear-Medicine Staff. *Appl. Sci.* **2023**, *13*, 9182. [CrossRef]
52. JCS Joint Working Group. Guidelines for Clinical Use of Cardiac Nuclear Medicine (JCS 2010). *Circ. J.* **2012**, *76*, 761–767. [CrossRef]
53. Hattori, K.; Inaba, Y.; Kato, T.; Fujisawa, M.; Yasuno, H.; Yamada, A.; Haga, Y.; Suzuki, M.; Zuguchi, M.; Chida, K. Evaluation of a New Real-Time Dosimeter Sensor for Interventional Radiology Staff. *Sensors* **2023**, *23*, 512. [CrossRef]
54. RaySafe i3—Instructions for Use. 2020. Available online: https://www.raysafe.com/sites/default/files/2020-10/RaySafe%20i3%20Instructions%20for%20Use%20%28multilingual%29_0.pdf (accessed on 8 October 2025).
55. International Atomic Energy Agency. *Manual for First Responders to a Radiological Emergency*; Emergency Preparedness and Response; International Atomic Energy Agency: Vienna, Austria, 2006.
56. Chida, K. What Are Useful Methods to Reduce Occupational Radiation Exposure among Radiological Medical Workers, Especially for Interventional Radiology Personnel? *Radiol. Phys. Technol.* **2022**, *15*, 101–115. [CrossRef]
57. Inaba, Y.; Hitachi, S.; Watanuki, M.; Chida, K. Radiation Eye Dose for Physicians in CT Fluoroscopy-Guided Biopsy. *Tomography* **2022**, *8*, 438–446. [CrossRef]
58. Konta, S.; Ohno, S.; Shindo, R.; Yamamoto, K.; Haga, Y.; Kato, T.; Sota, M.; Kaga, Y.; Abe, M.; Chida, K. Assessment of Lens Absorbed Dose by Radiological Technologists during Mobile X-Ray Radiography: A Comparison between Computed Radiography and Flat Panel Detector Systems. *Radiol. Phys. Technol.* **2025**, *18*, 766–774. [CrossRef]
59. Ohno, S.; Shindo, R.; Konta, S.; Yamamoto, K.; Inaba, Y.; Chida, K. Radiation Exposure to the Brains of Interventional Radiology Staff: A Phantom Study. *Bioengineering* **2024**, *11*, 1083. [CrossRef]
60. Sagehashi, K.; Haga, Y.; Takahira, S.; Tanabe, M.; Nakamura, M.; Sota, M.; Kaga, Y.; Abe, M.; Tada, N.; Chida, K. Evaluation of Radiation Dose to the Lens in Interventional Cardiology Physicians before and after Dose Limit Regulation Changes. *J. Radiol. Prot.* **2024**, *44*, 031512. [CrossRef]
61. Haga, Y.; Chida, K.; Kaga, Y.; Sota, M.; Meguro, T.; Zuguchi, M. Occupational Eye Dose in Interventional Cardiology Procedures. *Sci. Rep.* **2017**, *7*, 569. [CrossRef] [PubMed]
62. Penfold, S.N.; Marcu, L.; Lawson, J.M.; Asp, J. Evaluation of physician eye lens doses during permanent seed implant brachytherapy for prostate cancer. *J. Radiol. Prot.* **2012**, *32*, 339. [CrossRef] [PubMed]
63. Inaba, Y.; Jingu, K.; Fujisawa, M.; Otomo, K.; Ishii, H.; Kato, T.; Murabayashi, Y.; Suzuki, M.; Zuguchi, M.; Chida, K. Evaluation of Radiation Doses Received by Physicians during Permanent 198Au Grain Implant Brachytherapy for Oral Cancer. *Appl. Sci.* **2024**, *14*, 6010. [CrossRef]

64. Higley, B.; Smith, F.W.; Smith, T.; Gemmell, H.G.; Gupta, P.D.; Gvozdanovic, D.V.; Graham, D.; Hinge, D.; Davidson, J.; Lahiri, A. Technetium-99m-1,2-Bis[Bis(2-Ethoxyethyl) Phosphino]Ethane: Human Biodistribution, Dosimetry and Safety of a New Myocardial Perfusion Imaging Agent. *J. Nucl. Med.* **1993**, *34*, 30–38. [PubMed]
65. Günay, O.; Sarıhan, M.; Yarar, O.; Abuqbeitah, M.; Demir, M.; Sönmezoğlu, K.; Abamor, E.; Kara, Ö.E.; İpek Işıkcı, N.; Aközcan, S.; et al. Determination of Radiation Dose from Patients Undergoing Tc-99m Sestamibi Nuclear Cardiac Imaging. *Int. J. Environ. Sci. Technol.* **2019**, *16*, 5251–5258. [CrossRef]